Universität Potsdam

Christine Böckmann, Jens Biele, Roland Neuber,
Jenny Niebsch

Retrieval of multimodal aerosol size distribution by inversion of multiwavelength data

NLD Preprints ; 38

Retrieval of Multimodal Aerosol Size Distribution by Inversion of Multiwavelength Data

Ch. Böckmann[a] J. Biele[b], R. Neuber[b] and J. Niebsch[c]

[a]Universität Potsdam, Institut für Mathematik, Postfach 601553
Potsdam D-14415 Germany

[b]Alfred Wegener Institute for Polar and Marine Research, Postfach 600149
Potsdam D-14401 Germany

[c]Weierstraß Institut für Angewandte Analysis und Stochastik, Mohrenstr. 39
Berlin D-10117 Germany

ABSTRACT

The ill-posed problem of aerosol size distribution determination from a small number of backscatter and extinction measurements was solved successfully with a mollifier method which is advantageous since the ill-posed part is performed on exactly given quantities, the points r where $n(r)$ is evaluated may be freely selected. A new two-dimensional model for the troposphere is proposed.

Keywords: Multiwavelength LIDAR, aerosol size distribution, ill-posed problem, inversion, mollifier method, coated and absorbing aerosols

1. INTRODUCTION

Atmospheric aerosols play an important role in many atmospheric processes, e.g. in the complex processes of tropospheric ozone production and of stratospheric ozone destruction. Aerosols provide surfaces for example for chemical reactions which activate Cl from CFCs. One of the key aspects in a further understanding of the importance of aerosols is the investigation of the spatial and temporal variability of their microphysical properties, e.g. parameters describing their mean size and surface-area concentration, see [Weidauer et al] Ref. 1. The problem of determining the aerosol size distribution function $n(r)$, by multispectral lidar measurements, belongs to the class of problems in mathematics called nonlinear inverse ill-posed problems.

2. MULTIWAVELENGTH LIDAR FOR AEROSOL INVESTIGATIONS

2.1. Scattering processes

The scattering of light by aerosols depends on their abundance, size distribution, composition and phase. As typical atmospheric aerosols have sizes in the range from 0.1 micron to several microns, their size is comparable to the wavelength of light. Therefore, their scattering and extinction properties show a wavelength dependence. This allows to investigate the properties of aerosols by the observation of backscattered light from laser pulses (lidar principle at various wavelengths). A multi channel detector collects the backscattered photons simultaneously on the emitted wavelengths and on others corresponding to inelastic backscattering. The elastic backscatter signal at the emitted wavelengths usually depends on the Rayleigh and Mie scattering processes only. (Absorption by trace gases will be neglected here.) Therefore they carry information about the air density (Rayleigh or molecular scattering) and about the aerosol backscatter coefficient (from aerosol scattering, which in simple cases can be described by Mie's theory). This is described by the "lidar equation" given in formula (1).

Other author information: (Send correspondence to Ch.B.)
Ch.B.: Email: bockmann@rz.uni-potsdam.de; Telephone: ++49-331-977-1476; Fax: ++49-331-977-1001
J.B.: Email: jbiele@awi-potsdam.de; Telephone: ++49-331-288-2133; Fax: ++49-331-288-2137
R.N.: Email: neuber@awi-potsdam.de; Telephone: ++49-331-288-2129; Fax: ++49-331-288-2137
J.N.: Email: niebsch@wias-berlin.de; Telephone: ++49-30-2037-7474; Fax: ++49-30-2044975

The inelastic backscatter signals originate from vibrational Raman scattering with the water, nitrogen and/or oxygen molecules of the atmosphere. They are recorded simultaneously with the corresponding elastic backscatter signals. While the Raman scattering process itself does not produce information about aerosols, the light intensities available for Raman scattering depend on the extinction experienced on the way between the light source (laser), the Raman scattering altitude, and the detector. Therefore the aerosol extinction coefficient can be obtained from these observations.

The purpose of aerosol investigations by lidar are to determine properties of the aerosols, which are deductible from their optical effects. In equations (1), (2), and (3), which describe the scattering and extinction processes, the particle number densities $n(r)$ (r is the particle radius and $n(r)$ describes the size distribution function) and the refractive index m appear. The problem of inverting the lidar equation is to obtain these functions from measured lidar data. Until recently this was done by assuming a shape of the size distribution function, usually a log-normal distribution, and by calculating according to Mie's theory synthetic lidar data at the wavelengths used. A fitting procedure is then employed to determine, which set of parameters describes the measured data best, see e.g. [Hamill et al] Ref. 2, [Larsen] Ref. 3, [Beyerle] Ref. 4, [Stein] Ref. 5. As this procedure depends on a priori assumptions, it is not satisfactorily and we want to present an alternative here.

2.2. Experimental set up

A multiwavelength aerosol lidar, as it is used by the Alfred Wegener Institute at the German Arctic station on Spitsbergen, employs wavelengths as given in the following Table 1. Wavelengths denoted with * are the corresponding

Table 1. Typical wavelengths employed in a multi wavelength lidar system.

laser type	wavelengths in nm
XeCl excimer	308, 332*, 353, 385*
Nd YAG	532, 607*, 1064
titanium sapphire	779

nitrogen Raman lines. The backscattered signals at 532 nm are also analysed with respect to their polarisation characteristics. The lasers emit pulses alternately and their signals are recorded simultaneously in a multiwavelength detector. A typical altitude resolution is 30 m and signals are accumulated for 1 min before storage on a computer.

2.3. Depolarisation measurements

As the laser light at 532 nm is linearly polarised, we can determine the depolarisation characteristics of the involved scattering processes. The small depolarisation effect of Rayleigh scattering is well known, see [Young] Ref. 6. The depolarisation effect of aerosol scattering depends on the shape of the particles. According to Mie's theory, spherical, homogeneous particles do not change the polarisation state of the incident radiation. However, as soon as the particles become aspherical or inhomogeneous, the polarisation state of the scattered light changes with respect to that of the incident light. This effect is used here to discriminate measurements of aerosol scattering at spherical and non-spherical particles.

2.4. Refractive index

The scattering and extinction coefficients of aerosols depend on their refractive index, which in turn reflects the material composition. In the case of stratospheric aerosols, only a limited number of compositions have to be considered. Volcanic aerosols consist of sulphuric acid, which condenses following the oxidation of gaseous sulphuric dioxide. This is by far the main component of stratospheric aerosols, as solid volcanic material sediments already after a very short time after a volcanic eruption event. Accordingly also the stratospheric background aerosol layer consists of sulphuric acid (the Junge layer). The refractive index of these aerosols can be calculated by the Lorentz-Lorenz formula from known atmospheric temperatures and water contents. In the stratosphere of the polar regions at least two more types of aerosols exist, so called Polar Stratospheric Clouds of types I and II. Type II consists of

water ice only, of which again the refractive index is known. Type I PSCs contain various mixtures of water, nitric acid, and sulphuric acid. Expressions to calculate their compositions have recently been published by [Carslaw et al] Ref. 7 and a calculation of the corresponding refractive indices can be found in [Luo et al] Ref. 8. For all of the stratospheric aerosols mentioned, however, the imaginary part of the refractive index is in the order of $10E-6$ and can therefore be neglected. For tropospheric aerosols the situation is different. They appear in a multitude of classes and many of them contain black materials like soot, which are good absorbers and therefore have imaginary parts of their refractive indices, which can exceed 0.05.

3. NUMERICAL SMOOTHED INVERSION

3.1. Inversion of backscatter and extinction integral equation in the stratosphere

3.1.1. Description of the problem

The mathematical model for such a LIDAR messuring process consists of one nonlinear and two linear integral equations. These are the LIDAR equation

$$P(\lambda,z) \;=\; C(\lambda)\; P_e(\lambda)\; \beta(\lambda,z)\; \frac{1}{z^2}\; \exp\{-2\int_{z_0}^{z} \alpha(\lambda,z')dz'\}\;, \tag{1}$$

(where λ is the wavelenght, z the height, C is a specific quantity of the messuring apperatus, P_e the intensity of the emitted signal, P the intensity of the detected signal, β is the backscattering coefficient, α the extinction coefficient) and the Fredholm integral equations of the first kind for backscattering and extinction coefficients β^{Aer} and α^{Aer}

$$\beta^{Aer}(\lambda,z) \;=\; \int_{r_a}^{r_b} K_\pi(r,\lambda;m)\; n(r,z)\; dr \;=\; \int_{r_a}^{r_b} \pi\; r^2\; Q_\pi(r,\lambda;m)\; n(r,z)\; dr\;, \tag{2}$$

$$\alpha^{Aer}(\lambda,z) \;=\; \int_{r_a}^{r_b} K_{ext}(r,\lambda;m)\; n(r,z)\; dr \;=\; \int_{r_a}^{r_b} \pi\; r^2\; Q_{ext}(r,\lambda;m)\; n(r,z)\; dr\;, \tag{3}$$

where r is the particle radius, m the refractive index, n the aerosol size distribution we are looking for, K_π the backscattering and K_{ext} the extinction kernel. We have $\beta=\beta^{Aer}+\beta^{Ray}$ and $\alpha=\alpha^{Aer}+\alpha^{Ray}$ with known β^{Ray} and α^{Ray}.

We want to consider the kernel functions K_π and K_{ext} of these integral equations. The kernel function reflects shape and material composition of particles. We assume Mie-particles. Following formulas hold for extinction and backscattering cross sections, see [Bohren/Huffman] Ref. 9,

$$Q_\pi \;=\; \frac{1}{k^2r^2}\Big|\sum_{n=1}^{\infty}(2n+1)(-1)^n(a_n-b_n)\Big|^2 \tag{4}$$

$$Q_{ext} \;=\; \frac{2}{k^2r^2}\sum_{n=1}^{\infty}(2n+1)Re(a_n+b_n)\;. \tag{5}$$

The mathematician Hadarmard wrote: A mathematical problem is said to be well-posed if it has a unique solution and the solution depends continuously on the data. A problem which is not well-posed is said to be ill-posed.

The conclusion is simple. The application of standard numerical techniques might yield nonphysical "solutions". The integration with K_π in (2) and K_{ext} in (3) has a "smoothing" effect on n in the sense that high-frequency components, cusps and edges in n are "smoothed out" by integration. We can therefore expect that the reverse process, i.e. that computing n from β^{Aer} or α^{Aer}, will tend to amplify any high-frequency components in β^{Aer} or α^{Aer}.

First, we replace the original ill-posed problem of finding $n(r,z)$ by a new problem of finding $n_\gamma(r,z)$. The new problem is well-posed, depends on a parameter $\gamma>0$, and in the absence of noise in the data, is consistent with the original problem.

Second, in the presence of noise in the data, with a fixed value of the parameter $\gamma>0$, we solve the new problem - not the original one - which is stable with respect to perturbations in the data.

Any Fredholm integral equation of the first kind is inherently ill-posed, see also [Castelletto/Rastello] Ref. 10 for

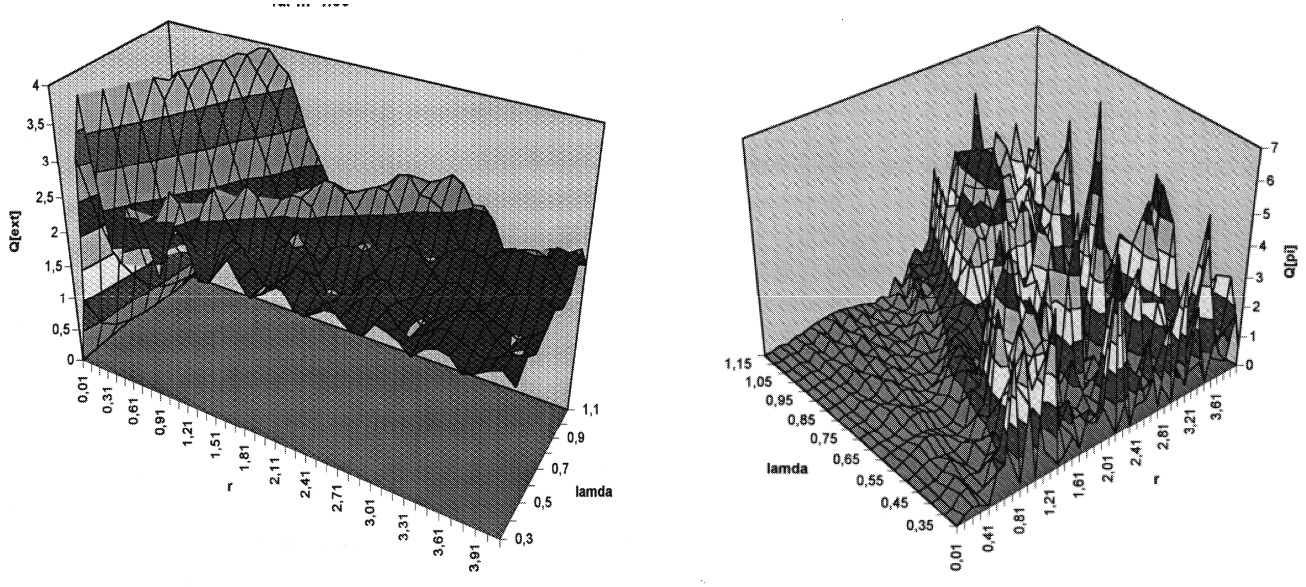

Figure 1. The functions (5) left and (4) right

a similar problem. The kernel functions in (2) and (3) are square integrable in $[r_a, r_b] \times [\lambda_a, \lambda_b]$. The degree of ill-posedness depends on the smoothness of the kernel function, i.e. the "smoother" the kernel K, the faster the singular values σ_i decay to zero (where smoothness is measured by the number of continuous partial derivatives of K). The degree of the decay is a measure for the ill-posedness of the operator, see [Hofmann] Ref. 11.
So the two integral equations (2) and (3) are extremly different from each other, see Fig. 1 and Fig. 2 (left). The degree of ill-posedness of (3) is higher.

3.1.2. The mollifier method

Now we want to answer the following question. Is it possible to form a reasoned estimate of inaccessible values of a function from a few indirect measurements? This is of course at the heart of inverse theory and the mollifier method is designed to provide such estimates.
The altitude z and the refractive index m are fixed values for the moment. Suppose N measurements $\mu_1, ..., \mu_N$. We start from

$$\mu(\lambda_j) \;=\; \int_{r_a}^{r_b} K(s, \lambda_j)\; n(s)\; ds, \quad j = 1, ..., N \tag{6}$$

or shorter expressed as a linear, continuous operator equation

$$\mu \;=\; K\; n \tag{7}$$

between Hilbert spaces X and Y, i.e.

$$K \;:\; X = L_2([r_a, r_b]) \;\rightarrow\; Y = R^N \;. \tag{8}$$

X is a space of functions and Y is a finite-dimensional space of measurements. We use $X = L_2([r_a, r_b])$ for a suitable intervall $[r_a, r_b] \subset R$. Suppose N measurements $\mu_1, ..., \mu_N$ are available which represent values of linearly independent functionals on an unknown function n. Now we replace the original ill-posed problem of finding $n(r)$ by a new well-posed problem of finding $n_\gamma(r)$, i.e. instead of n we compute the approximation n_γ with a suitable mollifier e_γ, thus reducing the high-frequency components in the solution which are mostly affected by the data noise. The idea is to estimate a smoothed version $n_\gamma(r) = E_\gamma\; n(r)$ of $n(r)$ by a linear combination

$$n_\gamma \;\simeq\; \varphi_{\gamma 1}\mu_1 + ... + \varphi_{\gamma N}\mu_N \tag{9}$$

by appropriately shaping the coefficients $\varphi_{\gamma 1}(r), ..., \varphi_{\gamma N}(r)$ which means that we have to compute the reconstruction kernel $\varphi_\gamma(r) \in R^N$ for all reconstruction points r. These values are precomputed independently of the data, i.e. the inversion operator is precomputed without using the data μ, see [Louis] Ref. 12. $\gamma > 0$ is the so called smoothing parameter acting as a regularization parameter. In order to obtain a stable approximation of $n(r)$, we select a smoothing operator E_γ with $\lim_{\gamma \to 0} E_\gamma n(r) = n(r)$, see [Louis/Maaß] Ref. 13. Then we have

$$\begin{aligned} E_\gamma\ n(r) &\simeq \sum_{j=1}^{N} \varphi_{\gamma j}(r)\ \mu_j \\ &= \sum_{j=1}^{N} \varphi_{\gamma j}(r) \int K(s,\lambda_j)\ n(s)\ ds \\ &= \int n(s)\ [\ \sum_{j=1}^{N} K(s,\lambda_j)\ \varphi_{\gamma j}(r)]\ ds \\ &= \int n(s)\ w_{\gamma N}(r,s)\ ds \quad \text{with} \quad w_{\gamma N}(r,s) = \sum_{j=1}^{N} K(s,\lambda_j)\ \varphi_{\gamma j}(r) \end{aligned}$$

and

$$n(r) \simeq \lim_{\gamma \to 0} \int n(s)\ w_{\gamma N}(r,s)\ ds\ .$$

The first motivation of the method is based on the following idea. We recognize, that for $\gamma = 0$ $w_{\gamma N}(r,s)$ has to approximate the delta distribution $\delta(r-s)$. We have to look for $\min \| w_N(r,s) - \delta(r-s) \|$. Since this problem can not be solved in the function space L_2, we replace the delta distribution by an approximation e_γ, the so called mollifier function.
The second motivation of the method, see [Louis/Maaß] Ref. 13, follows. A smoothing operator $E_\gamma : L_2[r_a, r_b] \to L_2[r_a, r_b]$ with $\lim_{\gamma \to 0} E_\gamma n(r) = n(r)$ is selected and represented by

$$n_\gamma(r) = E_\gamma n(r) = \int e_\gamma(r,s)\ n(s)\ ds \quad \text{with} \quad e_\gamma(r,s) \simeq \sum_{j=1}^{N} \varphi_{\gamma j}(r) K(s,\lambda_j).$$

Then

$$n_\gamma(r) \simeq \sum_{j=1}^{N} \varphi_{\gamma j} \int K(s,\lambda_j)\ n(s)\ ds = \sum_{j=1}^{N} \varphi_{\gamma j}(r) \mu(\lambda_j).$$

Minimising the error leads to

$$|\ n_\gamma(r) - \sum_{j=1}^{N} \varphi_{\gamma j}(r) \mu(\lambda_j)\ | \leq \| n \| \left(\int (e_\gamma(r,s) - \sum_{j=1}^{N} \varphi_{\gamma j}(r) K(s,\lambda_j))^2\ ds \right)^{\frac{1}{2}}.$$

There are different possibilities for mollifier functions, e.g.

$$e_{\gamma 1}(x) = \frac{1}{2\gamma}\ \chi[-\gamma,\gamma] \quad \text{or} \quad e_{\gamma 2}(x) = \frac{1}{\pi\gamma}\ \mathrm{sinc}(\frac{1}{\gamma}x) \tag{10}$$

where χ is the characteristic function, here local averages of the solution are computed. The mollifier $e_{\gamma 2}$ is a band-limiting filter eliminating the high-frequency components in the solution, see Fig. 2. To get the coefficients $\varphi_{\gamma 1}(r), ..., \varphi_{\gamma N}(r)$ we have to minimise

$$\| \sum_{j=1}^{N} K(s,\lambda_j)\ \varphi_{\gamma j}(r) - e_\gamma(r-s) \|_{L^2(R)} \tag{11}$$

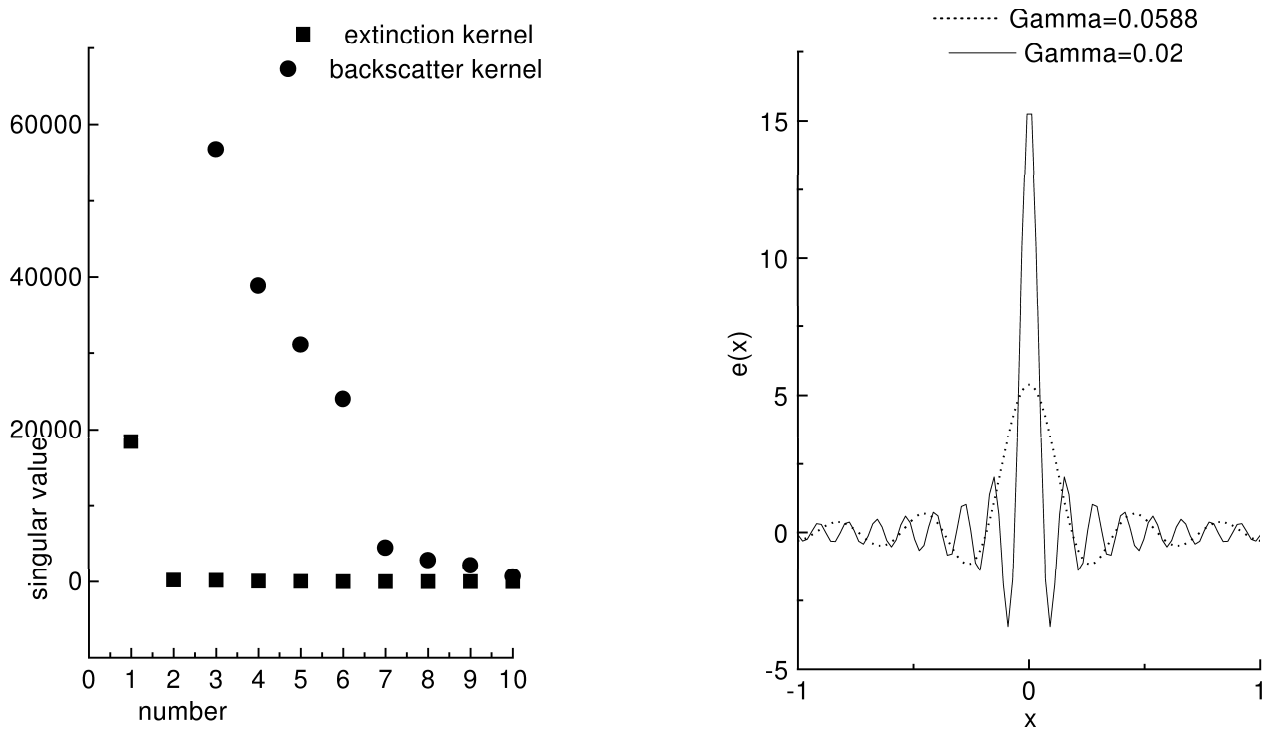

Figure 2. The degree of the decay (left) and the mollifier function $e_{\gamma 2}$ (right)

which is obviously minimised, see APPENDIX A, by $\varphi_\gamma(r)$ with

$$B\ \varphi_\gamma(r) \ = \ b_\gamma(r) \tag{12}$$

$$\text{where} \quad B_{ij} = \int_{r_a}^{r_b} K(s,\lambda_i)\ K(s,\lambda_j)\ ds \tag{13}$$

$$\text{and} \quad b_{\gamma j}(r) = \int_{r_a}^{r_b} K(s,\lambda_j)\ e_\gamma(r-s)\ ds. \tag{14}$$

It is important to mention that no artificial discretization of n is needed as introduced by projection methods, see [Böckmann] Ref. 14.

3.1.3. Application of mollifier method

Firstly, we carry out a simple application. There are given N_1 measurements of $\beta^{Aer}(\lambda_i^\beta), i = 1, ..., N_1$, and N_2 measurements of $\alpha^{Aer}(\lambda_j^\alpha), j = 1, ..., N_2$ with $\lambda^\beta = (308, 353, 532, 779, 1064)[nm]$ and $\lambda^\alpha = (332, 385, 532, 607)[nm]$. Then we have

$$n^\beta(r) \ = \ \sum_{i=1}^{N_1} \beta(\lambda_i^\beta)\varphi_{\gamma_1 i}^\beta(r) \quad \text{and} \quad n^\alpha(r) \ = \ \sum_{j=1}^{N_2} \alpha(\lambda_j^\alpha)\varphi_{\gamma_2 j}^\alpha(r) \tag{15}$$

with

$$\left[\begin{array}{c|c} B_\pi & 0 \\ \hline 0 & B_{ext} \end{array}\right] \left[\begin{array}{c} \varphi^\beta_{\gamma_1}(r) \\ \hline \varphi^\alpha_{\gamma_2}(r) \end{array}\right] = \left[\begin{array}{c} b^\pi_{\gamma_1}(r) \\ \hline b^{ext}_{\gamma_2}(r) \end{array}\right] \tag{16}$$

The reconstructed size distribution follows from

$$n(r) \;=\; \frac{1}{2}\,(n^\beta(r) \;+\; n^\alpha(r))\;. \tag{17}$$

We study two examples with

$$n_1(r) \;=\; \exp(-0.5\,\ln^2(r/r_{med})/\,\ln^2\sigma) \quad \text{and} \quad n_2(r) \;=\; \frac{1}{r}\,\frac{1}{\sqrt{2\pi}\,\ln\sigma}\,\exp(-0.5\,\ln^2(\frac{\frac{r}{r_{med}}}{\ln\sigma}))\;, \tag{18}$$

see [Grabowski/Latosinska] Ref. 15, where $r_{med} = 0.18$, $\sigma = 1.75$, $m = 1.4676$, $r_a = 0.001$ and $r_{b_1} = 1.0$ ($r_{b_2} = 0.5$). Reconstructions with $e_{\gamma 2}$ and $\gamma_\beta = \gamma_\alpha = 1/17$ for the first size distribution $n_1(r)$ are shown in Fig. 3 (left) with noisy data, 3% noise. We use a truncated singular value decompostion for the solution of the linear equation system

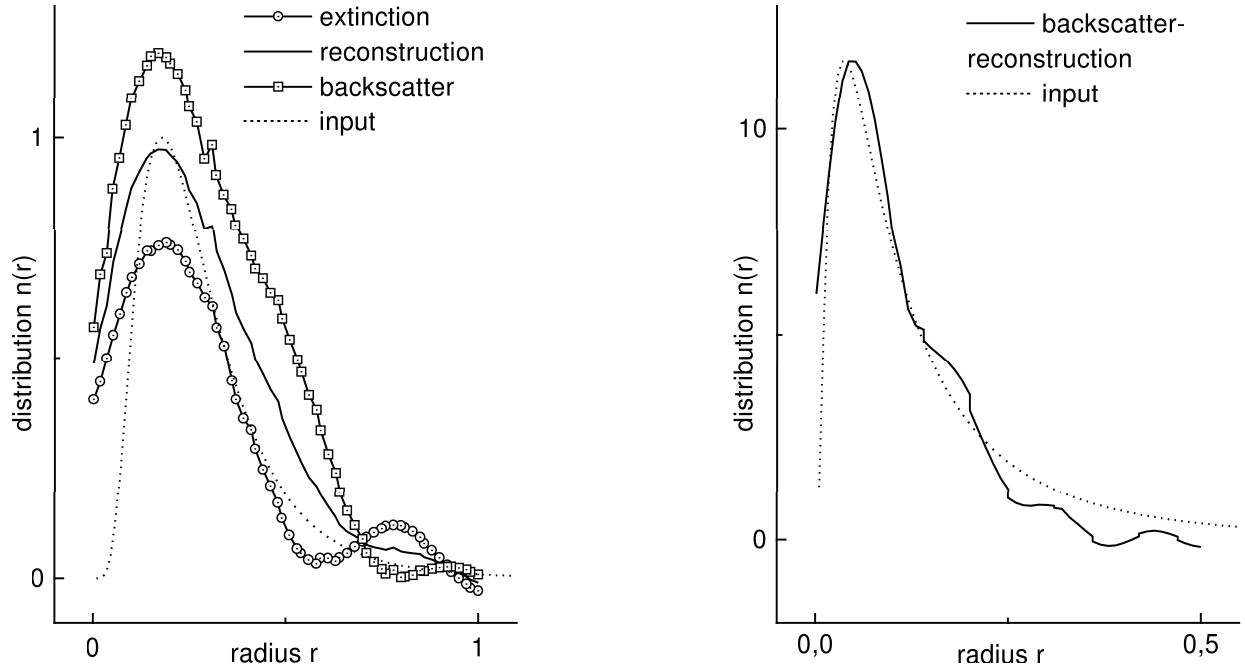

Figure 3. Numerical results with the simple method

(16). If we solve the block system seperatly, we recognize that for the backscatter system no truncation has to be used. But for the extinction system we have to truncate two singular values. The reason is the high degree of ill-posedness of equation (3). The discrete equation (16) inherits the instability of the integral operator, which means

that the matrix is ill-conditioned, see [Böckmann/Niebsch] Ref. 16. In fact of this, the $\varphi^{\alpha}_{\gamma_\alpha}$ are computed by using truncated singular value decomposition, i.e. by discrete regularization with a rather small regularization parameter. The fine regularization is achieved by the parameter γ in e_γ. The backscatter-reconstruction with $e_{\gamma 2}$ ($\gamma_\beta = 1/50$) and truncation of four singular values for the second size distribution $n_2(r)$ with exact data is shown in Fig. 3 (right). The extinction reconstruction was not successfull. The conclusion is that the inversion via the backscatter integral equation is more stable. It is important to mention that we do not require an initial size distribution, i.e. we start without a special shape of the size distribution and we execute no fit.
Secondly, we carry out a new connecting application. We take the same assumptions as before. There are N_1 measurements of $\beta(\lambda_i^\beta)$, $i = 1, ..., N_1$, N_2 measurements of $\alpha(\lambda_j^\alpha)$, $j = 1, ..., N_2$ and N_3 measurements of $\beta(\lambda_k^{\alpha\beta})$ and $\alpha(\lambda_k^{\alpha\beta})$, $k = 1, ..., N_3$ with $\lambda^\beta = (308, 353, 779, 1064)[nm]$, $\lambda^\alpha = (332, 385, 607)[nm]$ and $\lambda^{\alpha\beta} = (532)[nm]$. Now we describe a more general and connecting application. We have

$$\beta(\lambda_i^\beta) = \int K_\pi \; n(r) \; dr, \quad i = 1, ..., N_1 \tag{19}$$

$$\alpha(\lambda_j^\alpha) = \int K_{ext} \; n(r) \; dr, \quad j = 1, ..., N_2 \tag{20}$$

$$\beta(\lambda_k^{\alpha\beta}) + \alpha(\lambda_k^{\alpha\beta}) = \int (K_\pi \; + \; K_{ext}) \; n(r) \; dr, \quad k = 1, ..., N_3 \tag{21}$$

$$\tag{22}$$

or shorter expressed

$$\mu(\lambda_i) = \int \tilde{K} \; n(r) \; dr \tag{23}$$

with

$$\tilde{K} = \begin{cases} K_\pi & : \; \lambda_i \in \lambda^\beta \\ K_{ext} & : \; \lambda_i \in \lambda^\alpha \\ K_\pi \; + \; K_{ext} & : \; \lambda_i \in \lambda^{\alpha\beta} \end{cases}$$

Now it is possible to start the mollifier method again with

$$\tilde{B} \; \tilde{\varphi_\gamma}(r) = \tilde{b} \quad \text{and} \quad n(r) = \sum_{j=1}^{N} \tilde{\varphi_{\gamma_j}}(r) \; \mu(\lambda_j). \tag{24}$$

Computer simulations are running.

3.2. Inversion of backscatter and extinction integral equation in the troposphere

3.2.1. Description of the two-dimensional model for multimodal distributions

The determination of the aerosol size distribution in the troposphere is a problem which is a more extensive one. Since the tropospheric aerosol contains a large number of species, the model process is much more complicated than in the stratosphere. Aerorols of different compositions has different refractive indices m. The aerosol size distribution is a multimodal one. In general the number of different particles and their refractive indices are unknown.
In the case of a bimodal log-normal size distribution of one species with $m = 1.4 - 0.001i$ [Müller et al] Ref. 17 demonstrated a successfully simulated inversion with eight optical data points (six backscatter and two extinction coefficients) via Tikhonov-regularization, i.e. the inversion does not depend on the shape of the underlying size distribution. We want to generalize this model. We propose two possibilities for a new troposphere model. First, we describe a new simple model of superposition and second, a new two-dimensional model.
Firstly, we assume that we know the number k and the refractive indices m_i, $i = 1, ..., k$ of the k species. Now we model the first kind Fredholm integral equation as follows

$$\beta^{Aer}(\lambda) = \sum_{i=1}^{k} \int_{r_a}^{r_b} K_\pi(r, \lambda, m_i) \; n(r, m_i) \; dr$$

$$= \int_{r_a}^{r_b} \sum_{i=1}^{k} K_\pi(r,\lambda,m_i)\ n(r,m_i)\ dr$$

$$\simeq \int_{r_a}^{r_b} (\sum_{i=1}^{k} c_i\ K_\pi(r,\lambda,m_i))\ n(r)\ dr$$

$$\text{with} \quad n(r) = \sum_{i=1}^{k} n(r,m_i) \quad \text{and} \quad \sum_{i=1}^{k} c_i = 1\ ,$$

i.e. we approximate the problem via a convex combination, e.g. corresponding to the relative concentration or any other suitable criterion. The equation for α^{Aer} is treated in the same way. As result we get an approximative function $n(r)$ which represents the superposition of the size distributions of the k different species.
Secondly, in general the number k of different species and their refractive indices m_i, $i = 1, ..., k$ are unknown. From mathematical view, now we have to solve a two-dimensional ill-posed problem

$$\beta^{Aer}(\lambda) = \int_{r_a}^{r_b}\int_{m_a}^{m_b} K_\pi(r,\lambda,m)\ n(r,m)\ dm\ dr \quad \text{and} \quad \alpha^{Aer}(\lambda) = \int_{r_a}^{r_b}\int_{m_a}^{m_b} K_{ext}(r,\lambda,m)\ n(r,m)\ dm\ dr \quad (25)$$

in the form of two Fredholm integral equations. This problem can be solved by a two-dimensional mollifier method. The result, first in the absence of noise in the data, is a two-dimensional size distribution function $n(r,m)$. We obtain from this function the number k of different species, the refractive indices m_i, $i = 1, ..., k$, and the size distributions $n(r,m_i)$, $i = 1, ..., k$ of the different species.

3.3. The kernel functions K_π and K_{ext}

To determine the size distribution of particles in the troposphere and stratosphere with LIDAR mesurements we have to make assumptions about the shape and material composition (e.g. the refractive index). These properties are reflected in the kernel functions K_π and K_{ext}. We consider spherical particles which can be inhomogeneous and absorbing. Absorbing particles exist in the troposphere. For absorbing particles the refractive index is complex. We model the inhomogeneities considering core and cover of a spherical particle and different layers between both, see [Kerker] Ref. 18. [Stämpfli et al] Ref. 19 showed that for Polar Stratospheric Clouds (PSC) of type II the kernel function for the inhomogeneous model is different from that for the homogeneous model, see Fig. 4. Thus we can not neglegt the model influence.
If there are light pollutions in the core we hardly have differences to the nonabsorbing model. But additional light pollutions in the cover lead to a visible decrease for the backscattering efficiency K_π, see Fig. 5.
In Fig. 4 (right) K_{ext} is represented consisting of a nitrit acid trihydrate (NAT) core ($m[1] = 1.5, r[1] = 1\mu m$) and a water ice cover ($m[2] = 1.31, r[2] = 1\mu m \ldots 6\mu m$). The wavelength is $0.9\mu m$. Here the average refractive index for the homogeneous case, see Fig. 4 (left), is determined by the Lorentz-Lorenz formula.
In Fig. 5 (left) K_π is shown as above and on the right hand side the refractive indices are changed to $m[1] = 1.5 + 0.01i, m[2] = 1.31 + 0.01i$.
Even for light pollutions we get this big difference. Small soot inclusions in the core can be highly absorbing. An imaginary component of 0.05 is not extreme, see [Baumgardner et al] Ref. 20. Since especially tropospheric aerosol consists of absorbing particles, it is very important to have an absorbing model (e.g. algorithms for complex inputs) especially for K_π, as we see in Fig. 5 (right).

APPENDIX A. DERIVATION OF EQUATION (12)

We have to minimize

$$|| \sum_{j=1}^{N} K(s,\lambda_j)\varphi_{\gamma j}(r) - e_\gamma(r-s)||_{L^2(R)} = \left(\int_{r_a}^{r_b} \left[\sum_{j=1}^{N} K(s,\lambda_j)\varphi_{\gamma j}(r) - e_\gamma(r-s) \right]^2 ds \right)^{\frac{1}{2}} ,$$

i.e.

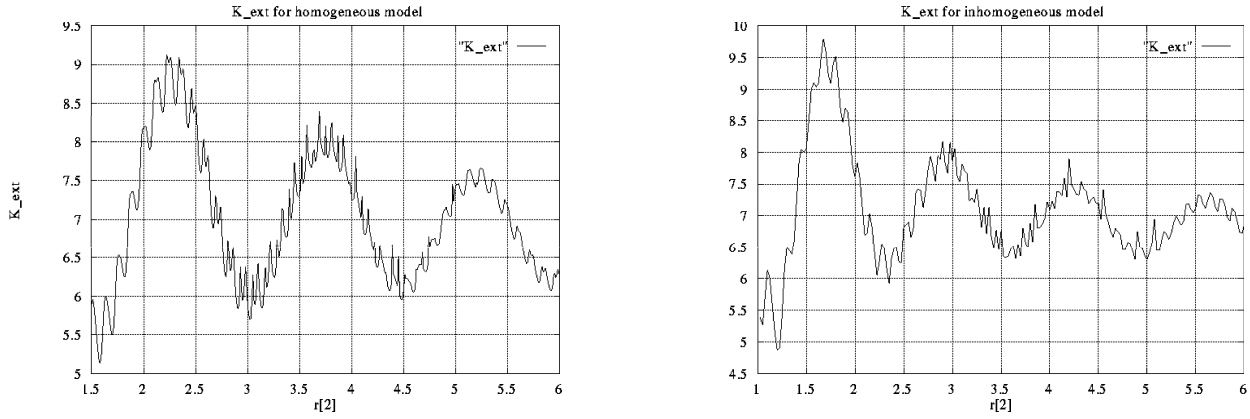

Figure 4. Homogeneous model (left) and inhomogeneous model (right)

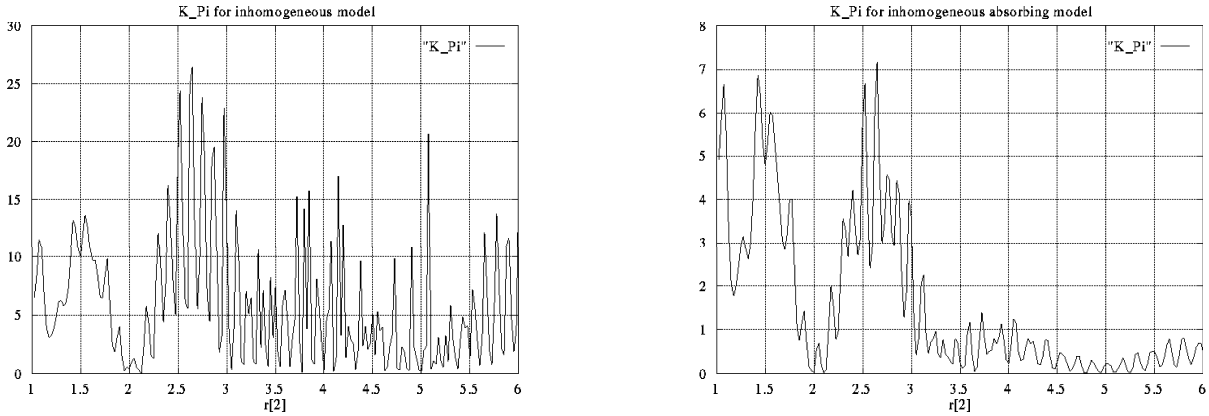

Figure 5. Inhomogeneous nonabsorbing model (left) and light absorbing core and cover (right)

$$Z = \frac{1}{2} \int_{r_a}^{r_b} \left[\sum_{j=1}^{N} K(s, \lambda_j) \varphi_{\gamma j}(r) - e_\gamma(r-s) \right]^2 ds$$

The necessary conditions are

$$\frac{\partial Z}{\partial \varphi_{\gamma 1}} = \int_{r_a}^{r_b} \left[\sum_{j=1}^{N} K(s, \lambda_j) \varphi_{\gamma j}(r) - e_\gamma(r-s) \right] \cdot K(s, \lambda_1) ds = 0$$

$$\vdots$$

$$\frac{\partial Z}{\partial \varphi_{\gamma N}} = \int_{r_a}^{r_b} \left[\sum_{j=1}^{N} K(s, \lambda_j) \varphi_{\gamma j}(r) - e_\gamma(r-s) \right] \cdot K(s, \lambda_N) ds = 0$$

This leads to the following linear equation system

$$\begin{bmatrix} \int_{r_a}^{r_b} K(s,\lambda_1)K(s,\lambda_1)ds & \dots & \int_{r_a}^{r_b} K(s,\lambda_1)K(s,\lambda_N)ds \\ \vdots & & \vdots \\ \int_{r_a}^{r_b} K(s,\lambda_N)K(s,\lambda_1)ds & \dots & \int_{r_a}^{r_b} K(s,\lambda_N)K(s,\lambda_N)ds \end{bmatrix} \begin{bmatrix} \varphi_{\gamma 1} \\ \vdots \\ \varphi_{\gamma N} \end{bmatrix} = \begin{bmatrix} \int_{r_a}^{b} e_\gamma(r-s)K(s,\lambda_1)ds \\ \vdots \\ \int_{r_a}^{r_b} e_\gamma(r-s)K(s,\lambda_N)ds \end{bmatrix}$$

REFERENCES

1. D. Weidauer et al, "Ozone, VOC, NO_2 and aerosol monitoring in urban and industrial areas using a mobile DIAL system," in *Advances in Atmospheric Remote Sensing with Lidar*, A. Ansmann et al, ed., pp. 423–426, Springer, New York, Berlin, Heidelberg, 1996.
2. P. Hamill et al, "An analysis of various nucleation mechanisms for sulfate particles in the stratosphere," *J. Aerosol Sci.* **13**, pp. 561–585, 1982.
3. N. Larsen, "Stratospheric aerosols, backscatter measurements from thule, european arctic stratospheric ozone experiment," *Report, Danish Meteorological Institute* **1**, 1992.
4. G. Beyerle, "Multiwavelength lidar measurements of stratospheric volcanic aerosols and polar stratospheric clouds on Spitsbergen (79°N, 12°E)," *Reports on Polar Research, Alfred Wegener Institute* **138**, 1994.
5. B. Stein, "Charakterisierung von stratosphaerischen Aerosolen mit multispektralem Lidar," *Diss., Free University of Berlin* , 1994.
6. A. T. Young, "Rayleigh scattering," *Appl. Optics* **20**, pp. 533–535, 1981.
7. K. S. Carslaw et al, "An analytic expression for the composition of aqueous HNO_3-H_2SO_4 stratospheric aerosols including gas phase removal of HNO_3," *Geophys. Res. Lett.* **22**, pp. 1877–1880, 1995.
8. B. Luo et al, "Densities and refractive indices of $H_2SO_4/HNO_3/H_2O$ solutions at stratospheric temperatures," *Geophys. Res. Lett.* **23**, pp. 3707–3710, 1996.
9. G. F. Bohren and D. R. Huffman, *Absorption and Scattering of Light by Small Particles*, John Wiley and Sons, New York, 1983.
10. S. Castelletto and M. Rastello, "Photon flux measurements by regularised solution of integral equations," in *Advanced Mathematical Tools in Metrology III*, P. Ciarlini et al, ed., World Scientific, Singapore, 1997.
11. B. Hofmann, *Regularization for Applied Inverse and Ill-Posed Problems*, BSB Teubner, Leipzig, 1986.
12. A. K. Louis, "Approximate inverse for linear and some nonlinear problems," *Inverse Problems* **12**, pp. 175–190, 1996.
13. A. K. Louis and P. Maaß, "A mollifier method for linear operator equations of the first kind," *Inverse Problems* **6**, pp. 427–440, 1990.
14. C. Böckmann, "Projection method for lidar measurements," in *Advanced Mathematical Tools in Metrology III*, P. Ciarlini et al, ed., World Scientific, Singapore, 1997.

15. J. Grabowski and M. Latosinska, "The evaluation of a backscattering lidar for measurements of air polution concentration profiles and particulate emissions from single stacks - computer simulations," in *Chemical Industry and Environment II*, N. Piccinini and R. Delorenzo, eds., *Air Pollution Water Treatment* **1**, pp. 41–48, 1996.
16. C. Böckmann and J. Niebsch, "Mollifier methods for aerosol size distribution," in *Advances in Atmospheric Remote Sensing with Lidar*, A. Ansmann et al, ed., pp. 67–70, Springer, New York, Berlin, Heidelberg, 1996.
17. D. Müller et al, "Retrieval of microphysical particle properties from backscatter and extinction data by inversion via regularization," in *Optical Remote Sensing of the Atmosphere*, Optical Society of American Washington DC, ed., *OSA Technical Digest Series* **5**, pp. 94–96, 1997.
18. M. Kerker, *The Scattering of Light and other electromagnetic radiation*, Academic Press, New York and London, 1969.
19. P. Stämpfli et al, "Scattering properties of inhomogeneous polar stratospheric clouds," *Personal communication* , 1995.
20. D. Baumgardner et al, "Refractive indices of aerosols in the upper troposphere and lower stratosphere," *Geophysical Research Letters* **23**, pp. 749–752, 1996.